JOURNAL OF NATURAL PRODUCTS

Article

pubs.acs.org/jnp

Anti-Neurodegenerative Biflavonoid Glycosides from *Impatiens balsamina*

Chung Sub Kim,[†] Munhyung Bae,[‡] Joonseok Oh,[§,⊥] Lalita Subedi,[∥,□] Won Se Suh,[†] Sang Zin Choi,[#] Mi Won Son,[#] Sun Yeou Kim,[∥,□] Sang Un Choi,[¶] Dong-Chan Oh,[‡] and Kang Ro Lee*[,†]

[†]Natural Products Laboratory, School of Pharmacy, Sungkyunkwan University, Suwon 16419, Republic of Korea
[‡]Natural Products Research Institute, College of Pharmacy, Seoul National University, Seoul 08826, Republic of Korea
[§]Department of Chemistry, Yale University, New Haven, Connecticut 06520, United States
[⊥]Chemical Biology Institute, Yale University, West Haven, Connecticut 06516, United States
[∥]Gachon Institute of Pharmaceutical Science, Gachon University, Incheon 21936, Republic of Korea
[□]College of Pharmacy, Gachon University, #191, Hambakmoero, Yeonsu-gu, Incheon 21936, Republic of Korea
[#]Dong-A ST Research Institute, Kiheung, Yongin 17073, Republic of Korea
[¶]Korea Research Institute of Chemical Technology, Daejeon 34114, Republic of Korea

Supporting Information

ABSTRACT: Four biflavonoid glycosides, balsamisides A–D (**1**–**4**), and nine known compounds (**5**–**13**) were obtained from the white petals of *Impatiens balsamina*. The 2D structures of the purified phytochemicals were established using conventional NMR techniques in addition to the new long-range HSQMBC NMR experiment. Acid hydrolysis followed by experimental and quantum-mechanics-based ECD data analysis permitted full configurational assignment of the purified metabolites. Compounds **1**–**13** were assessed for their potential to impede the generation of nitric oxide in lipopolysaccharide-stimulated BV2 cells. They were also investigated for potential neuroprotective activity using C6 cells and cytotoxicity against some human tumor cell lines, but were inactive (IC_{50} > 10 μM) against all the cell lines.

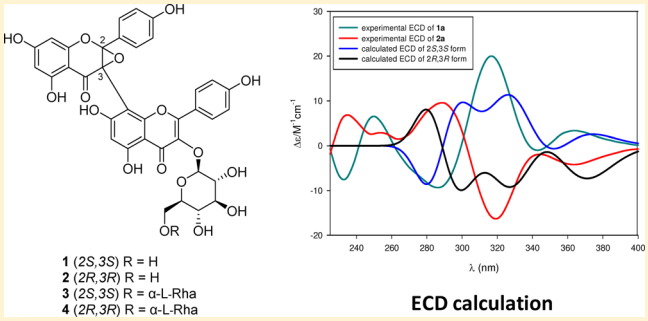

Impatiens balsamina L. (Balsaminaceae) is commonly called "Rose Balsam" or "Garden Balsam" and inhabits Korea, China, and India. For centuries, this annual herbaceous plant has been employed as a Chinese folk medicine, and, in particular, the flowers have been employed for the effective control of dermatitis, lumbago, neuralgia, burns, and scalds.[1] According to published research, the extracts of the *I. balsamina* petals showed antinociceptive, antioxidative, and antitumor activities,[1−3] and several flavonoids and naphthoquinones were shown to be the predominant constituents exhibiting anti-inflammatory, antipruritic, and antianaphylactic activities.[4−6]

Many flavonoids exhibit neuroprotective and anti-inflammatory activities via multiple underlying mechanisms. Apigenin and diosmin showed potent anti-inflammatory properties by hampering nitric oxide (NO) production and tumor necrosis factor (TNF)-α release in microglia. The flavanone hesperetin showed protecting activity of cortical neurons from oxidative stress, neurotoxicity associated with amyloid β (Aβ), and excitotoxicity induced by glutamate. Flavonoids from the *Epimedium* genus exhibited neuroprotective activity by enhancing the expression of nerve growth factor (NGF).[7−9] Therefore, diverse flavonoid architectures could be developed into a structurally relevant pharmacophore for the treatment of neurodegenerative diseases since NO and NGF play important roles regulating inflammatory responses and ameliorating tissue damage related to brain injury.[10,11]

Preliminary screening showed that the EtOAc-soluble phase of the MeOH extract of the flowers of *I. balsamina* not only reduced NO levels in lipopolysaccharide (LPS)-stressed murine microglia BV2 cells (IC_{50} 5.3 μg/mL) but also triggered NGF secretion in C6 glioma cells (152.64 ± 3.91% at 50 μg/mL). This resulted in the purification and characterization of phenolic compounds showing anti-inflammatory and neuroprotective activities in a recent study.[12] In the current study, four new biflavonoid glycosides, balsamisides A–D (**1**–**4**), and nine known metabolites (**5**–**13**) were identified. The characterization of the structures of these new biflavonoids was carried out utilizing spectroscopic techniques such as conventional NMR approaches, together with a new heteronuclear experiment, long-range (LR)-HSQMBC, which explores the use of long-range $^{n}J_{CH}$ heteronuclear couplings.[13] The absolute

Received: October 25, 2016

DOI: 10.1021/acs.jnatprod.6b00981
J. Nat. Prod. XXXX, XXX, XXX−XXX

Chart 1

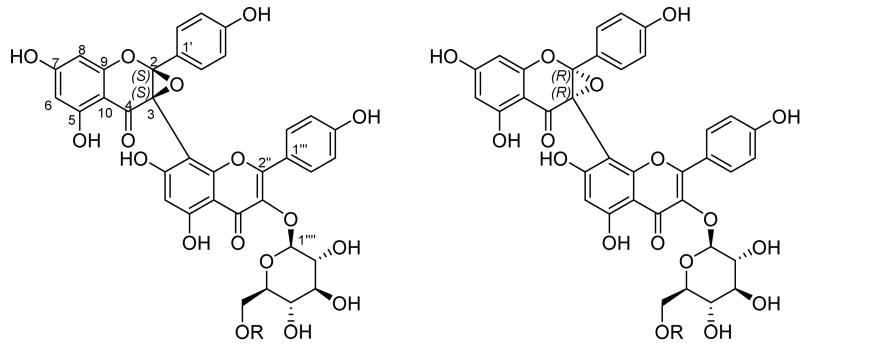

R
1 H
3 α-L-Rha

R
2 H
4 α-L-Rha

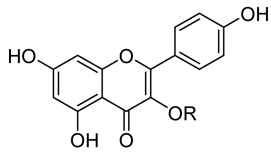

R
5 H
6 β-D-Glc
7 α-L-Rha-(1→2)-β-D-Glc
8 α-L-Rha-(1→6)-β-D-Glc
9 β-D-All

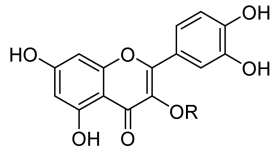

R
10 H
11 β-D-Glc
12 α-L-Rha-(1→6)-β-D-Glc

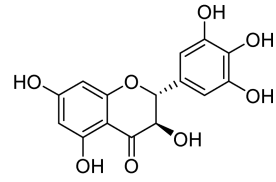

13

configurations were defined by comparison of experimental and computed electronic circular dichroism (ECD) data of the aglycones following acid hydrolysis. The purified compounds **1**−**13** were assessed for the hampering effects on NO generation from activated microglia and assessed for their potential neuroprotective activity via inducing NGF secretion from astrocytes and cytotoxicity against four cancer cell lines.

RESULTS AND DISCUSSION

The molecular formula of balsamiside A (**1**, yellowish gum) was confirmed based on the deprotonated molecular ion $[M - H]^-$ at *m*/*z* 731.1243 (calcd for $C_{36}H_{27}O_{17}$, 731.1243) in the HRFABMS spectrum and its ^{13}C NMR data. The ^1H NMR spectrum of **1** exhibited resonances characteristic for two 1,4-disubstituted phenyl groups [δ_H 8.17 (2H, d, *J* = 8.9 Hz), 7.38 (2H, d, *J* = 8.8 Hz), 6.93 (2H, d, *J* = 8.9 Hz), and 6.81 (2H, d, *J* = 8.8 Hz)], a 1,2,3,5-tetrasubstituted phenyl group [δ_H 5.98 (1H, d, *J* = 2.1 Hz) and 5.92 (2H, d, *J* = 2.1 Hz)], a 1,2,3,4,5-pentasubstituted phenyl group [δ_H 6.60 (1H, s)], and a *β*-glucopyranosyl moiety [δ_H 5.33 (1H, d, *J* = 7.6 Hz), 3.72 (1H, dd, *J* = 11.8, 2.3 Hz), 3.54 (1H, dd, *J* = 11.8, 5.8 Hz), 3.47 (1H, d, *J* = 8.9, 7.6), 3.43 (1H, t, *J* = 8.9 Hz), 3.32 (1H, dd, *J* = 9.8, 8.9 Hz), and 3.23 (1H, ddd, *J* = 9.8, 5.8, 2.3 Hz)]. The ^{13}C NMR spectrum of **1** displayed 30 resonances correlated to the aglycone motif and six to a *β*-glucopyranosyl moiety (δ_C 103.8, 78.6, 78.2, 75.9, 71.7, and 62.9). The 1D NMR data of **1** (Table 1) were analogous to those of 3-(quercetin-8-yl)-2,3-epoxy-flavanone except for the presence of the resonances associated with the hexopyranosyl residue in **1** and those of two 1,4-disubstituted phenyl groups in contrast to the two 1,3,4-trisubstituted phenyl functionalities reported in the known flavanone.[14] The location of the glucosidic residue was established to be at C-3″ based on the HMBC cross-peak between H-1‴″ and C-3″ (Figure 1). Structure **1** was elucidated via conventional 2D NMR experiments such as HSQC and HMBC data analysis (Figure 1).

The absence of hydrogens in the heterocyclic ring of the top unit in **1** poses a challenge not only for utilizing ROESY data to establish the relative configurations at C-2 and C-3 but for application of a chemical reaction for the determination of absolute configurations at C-2 and C-3. For the assignment of the absolute configuration of the 2,3-epoxide present in **1**, the experimental ECD spectrum of **1a** (hydrolysate of **1**) was compared to the simulated ECD spectra of the two plausible enantiomers of **1a** generated at the B3LYP/def-SV(P)//B3LYP/def-SV(P) level.[15,16] The experimental ECD spectrum of **1a** exhibited diagnostic positive Cotton effects at 363 and 317 nm, presumably attributed to the *p*-substituted phenolic motif, and a negative Cotton effect at 286 nm, caused by n → *π** excitation of the ketocarbonyl functionality, respectively. As illustrated in Figure 2, the simulated ECD spectrum of the (2*S*,3*S*)-enantiomer (**1a**) corresponded to the experimental ECD spectrum of **1a**. Consequently, the *S* absolute configurations of C-2 and C-3 in **1** were unequivocally assigned.

Acid hydrolysis of **1** afforded *β*-glucopyranose and the corresponding aglycone [(2*S*,3*S*)-2,3-epoxy-5,7,4′-trihydroxy-flavanone]-(3→8)-kaempferol (**1a**), whose ^1H NMR data closely matched those of 3-(kaempferol-8-yl)-2,3-epoxyflava-none, for which the absolute configuration was not assigned.[17] The D-configuration of the glucopyranose was established using

DOI: 10.1021/acs.jnatprod.6b00981
J. Nat. Prod. XXXX, XXX, XXX−XXX

Table 1. ^{1}H [ppm, mult., (J in Hz)] and ^{13}C NMR Spectroscopic Data of Compounds 1−4 in Methanol-d_4

	1		2		3		4	
pos.	δ_C	δ_H	δ_C	δ_H	δ_C	δ_H	δ_C	δ_H
2	119.7		119.6		119.6		119.6	
3	81.9		81.8		81.8		81.8	
4	192.6		192.3		192.5		192.3	
5	165.7		165.7		165.6		165.6	
6	98.2	5.98, d (2.1)	98.4	5.94, d (2.1)	98.2	5.96, d (2.1)	98.5	5.97, d (2.0)
7	169.7		169.8		169.8		170.3	
8	96.4	5.92, d (2.1)	96.6	5.90, d (2.1)	96.4	5.92, d (2.1)	96.7	5.91, d (2.0)
9	162.7		162.7		162.7		162.6	
10	100.3		100.1		100.3		100.3	
1′	125.3		125.4		125.3		125.4	
2′/6′	129.7	7.38, d (8.8)	129.8	7.39, d (8.9)	129.7	7.39, d (8.9)	129.8	7.39, d (8.8)
3′/5′	116.0	6.81, d (8.8)	116.0	6.81, d (8.9)	116.0	6.81, d (8.9)	116.0	6.81, d (8.8)
4′	160.3		160.3		160.3		160.3	
2″	159.5		159.3		160.0		159.4	
3″	135.8		135.8		135.6		135.9	
4″	180.0		180.0		179.7		180.1	
5″	166.6[a]		166.6[a]		166.7[a]		166.6[a]	
6″	96.6	6.60, s	96.5	6.61, s	96.7	6.61, s	96.7	6.61, s
7″	167.5[a]		167.5[a]		167.5[a]		167.6[a]	
8″	108.1[b]		108.1[b]		108.1[b]		108.0[b]	
9″	153.7		153.7		153.7		153.8	
10″	107.7[b]		107.8[b]		107.7[b]		107.8[b]	
1‴	122.5		122.5		122.5		122.3	
2‴/6‴	133.2	8.17, d (8.9)	133.2	8.21, d (8.9)	133.2	8.18, d (8.9)	133.3	8.23, d (9.0)
3‴/5‴	116.1	6.93, d (8.9)	116.1	6.93, d (8.9)	116.1	6.93, d (8.9)	116.3	6.95, d (9.0)
4‴	162.1		162.1		162.0		162.1	
1⁗(Glc)	103.8	5.33, d (7.6)	103.8	5.39, d (7.7)	103.8	5.28, d (7.4)	104.4	5.17, d (7.8)
2⁗	75.9	3.47, dd (8.9, 7.6)	76.0	3.47, dd (9.0, 7.7)	76.0	3.46, overlap	75.8	3.49, overlap
3⁗	78.2	3.43, t (8.9)	78.2	3.43, t (9.0)	77.5	3.39, overlap	77.5	3.29, overlap
4⁗	71.7	3.32, dd (9.8, 8.9)	71.7	3.28, dd (9.7, 9.0)	72.1	3.21, overlap	71.5	3.32, overlap
5⁗	78.6	3.23, ddd (9.8, 5.8, 2.3)	78.7	3.20, ddd (9.7, 5.8, 2.3)	78.2	3.44, overlap	78.3	3.39, overlap
6⁗a	62.9	3.72, dd (11.8, 2.3)	62.8	3.69, dd (11.9, 2.3)	69.1	3.84, m	68.3	3.78, m
6⁗b		3.54, dd (11.8, 5.8)		3.48, dd (11.9, 5.8)		3.39, overlap		3.44, overlap
1⁗′(Rha)					102.8	4.52, d (1.4)	102.3	4.52, d (1.6)
2⁗′					72.3	3.57, dd (3.3, 1.4)	72.2	3.62, dd (3.5, 1.6)
3⁗′					72.5	3.49, dd (9.5, 3.3)	72.5	3.48, overlap
4⁗′					74.0	3.27, t (9.5)	74.1	3.26, t (9.5)
5⁗′					69.9	3.44, overlap	69.8	3.41, overlap
6⁗′					18.0	1.13, d (6.2)	18.0	1.08, d (6.2)

[a,b]Interchangeable resonances.

chiral derivatization and GC/MS analyses.[18] The structure of **1** was thus assigned as [(2*S*,3*S*)-2,3-epoxy-5,7,4′-trihydroxyflavanone]-(3→8)-kaempferol 3″-*O*-*β*-D-glucopyranoside.

Compound **2** (balsamiside B) was purified as a yellowish gum and had the same molecular formula, $C_{36}H_{28}O_{17}$, as **1** based on the deprotonated HRFABMS molecular ion [M − H]$^-$ at m/z 731.1242 (calcd for $C_{36}H_{27}O_{17}$, 731.1243) and its ^{13}C NMR data. The 1D NMR data of **2** (Table 1) were similar to those of **1** with small chemical shift differences for all the resonances (within 0.06 for ^{1}H and 0.3 ppm for ^{13}C NMR chemical shifts), suggesting that **2** was a diastereomer of **1**. This assumption was supported by the HMBC cross-peak from H-1⁗ to C-3″, verifying the location of the sugar moiety in **2** (Figure 1). Acid hydrolysis of **2** led to the generation of the biflavonoid aglycone (**2a**), whose ^{1}H NMR data were identical to those of **1a**, indicating that their 2D structures were identical. The experimental ECD spectra of **2a** and **1a** displayed opposite Cotton effects from 260 to 400 nm, confirming that **1a** and **2a** were enantiomeric (Figure 2). Therefore, the structure of **2** was established as [(2*R*,3*R*)-2,3-epoxy-5,7,4′-trihydroxyflavanone]-(3→8)-kaempferol 3″-*O*-*β*-D-glucopyranoside.

The molecular formula of balsamiside C (**3**) was assigned as $C_{42}H_{38}O_{21}$ based on the HRFABMS (m/z 877.1821 [M − H]$^-$; calcd for $C_{42}H_{37}O_{21}$, 877.1822) and ^{13}C NMR data. The ^{1}H and ^{13}C NMR spectra resembled those of **1** and **2**, implying their intimate structural similarities. The major differences involved the presence of an *α*-rhamnopyranosyl moiety deduced from the NMR resonances at δ_H 4.52 (1H, d, J = 1.4 Hz), 3.57 (1H, dd, J = 3.3, 1.4 Hz), 3.49 (1H, dd, J = 9.5, 3.4 Hz), 3.44 (1H, overlap), 3.27 (1H, t, J = 9.5 Hz), and 1.13 (3H, d, J = 6.2 Hz), and δ_C 102.8, 74.0, 72.5, 72.3, 69.9, and 18.0. The HMBC cross-peak from H-6⁗ to C-1′′′′′ confirmed the position of the *α*-rhamnopyranosyl motif at C-6⁗ (Figure 1). The full configurational analyses of **3** were implemented in a similar manner to that for **1**, confirming 2*S* and 3*S* configurations. Thus, the structure of compound **3** was assigned

DOI: 10.1021/acs.jnatprod.6b00981
J. Nat. Prod. XXXX, XXX, XXX−XXX

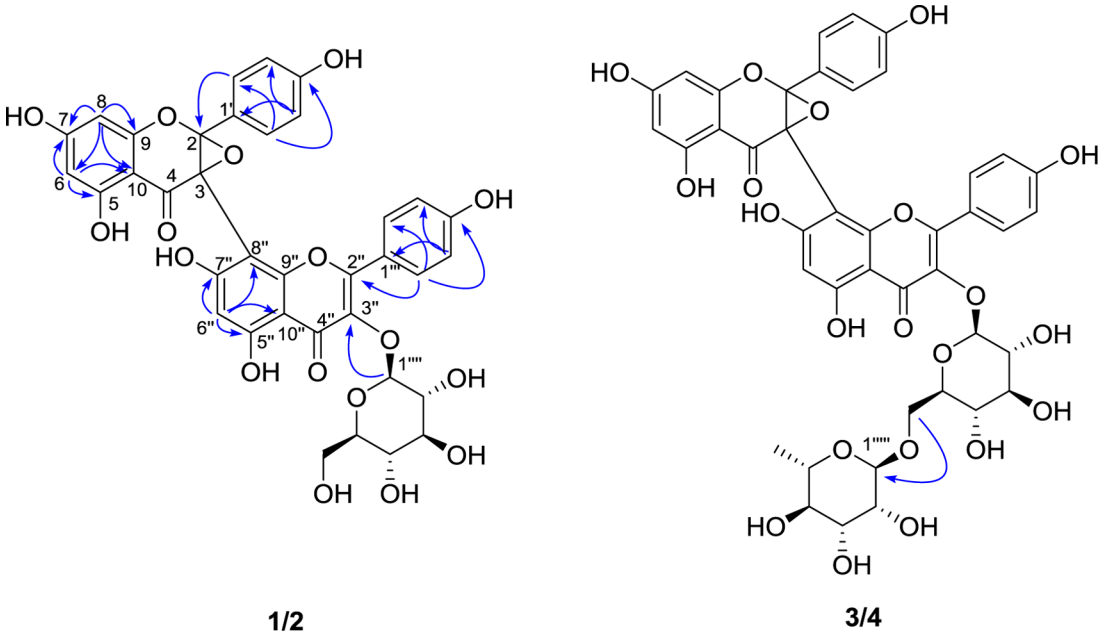

Figure 1. Key HMBC cross-peaks observed for compounds **1**−**4**.

as [(2*S*,3*S*)-2,3-epoxy-5,7,4′-trihydroxyflavanone]-(3→8)-kaempferol 3″-*O*-*α*-L-rhamnopyranosyl-(1→6)-*β*-D-glucopyranoside.

The molecular formula of **4** (balsamiside D) was established as $C_{42}H_{38}O_{21}$ via the HRFABMS ion at *m*/*z* 877.1823 ([M − H]$^-$; calcd for $C_{42}H_{37}O_{21}$, 877.1822), which is identical to that of **3**. Inspection of the 1D NMR information on **4** uncovered its structural resemblance to **3**. Indeed, analyses of the HSQC and HMBC NMR data confirmed that the structures **3** and **4** are highly similar. The 2*R* and 3*R* absolute configurations of **4** were corroborated using a similar approach to that for **1**. Therefore, the structure of **4** was identified as [(2*R*,3*R*)-2,3-epoxy-5,7,4′-trihydroxyflavanone]-(3→8)-kaempferol 3″-*O*-*α*-L-rhamnopyranosyl-(1→6)-*β*-D-glucopyranoside.

In order to corroborate the connectivity between the two flavonoid units in compounds **1**−**4**, the LR-HSQMBC experiment capable of detecting long-range correlations ($^{4-6}J_{CH}$) was used.[13] In the LR-HSQMBC spectrum of **3**, the cross-peaks from H-6″ to C-2 ($^5J_{CH}$), C-3 ($^4J_{CH}$), and C-4 ($^5J_{CH}$) were observed, indicating that the two flavonoid units were connected through a C-3−C-8″ bond (Figure 3). In addition, other long-range correlations involving H-6 and H-8/C-4, H-2′/C-3, H-6″/C-3″, C-4″, and C-9″, and H-2‴/C-3″ supported the NMR assignment of **3** (Figure 3). These data highlight the utility of the new heteronuclear experiment to afford unambiguous NMR assignments for a proton-deficient molecule.

The nine reported compounds were characterized as kaempferol (**5**),[19] kaempferol 3-*O*-*β*-D-glucopyranoside (**6**),[19] kaempferol 3-*O*-*α*-L-rhamnopyranosyl-(1→2)-*β*-D-glucopyranoside (**7**),[20] kaempferol 3-*O*-*α*-L-rhamnopyranosyl-(1→6)-*β*-D-glucopyranoside (**8**),[19] kaempferol 3-*O*-*β*-D-allopyranoside (**9**),[21] quercetin (**10**),[19] quercetin 3-*O*-*β*-D-glucospyranoide (**11**),[19] quercetin 3-*O*-*α*-L-rhamnopyranosyl-(1→6)-*β*-D-glucopyranoside (**12**),[22] and dihydromyricetin (**13**)[23] based on their observed and reported NMR data.

The anti-inflammatory effects of purified secondary metabolites (**1**−**13**) were assessed via the measurement of NO levels in the BV-2 cell line. The generation of NO in the cells was induced by the addition of the bacterial endotoxin LPS. As shown in Table 2, compounds **5** and **10** exhibited significant activities, possessing IC_{50}'s of 8.86 and 19.11 *μ*M, respectively, with insignificant cell toxicity at 20 *μ*M. The bioactivities were stronger than that of N^G-monomethyl-L-arginine (L-NMMA, positive control), exhibiting an IC_{50} value of 21.25 *μ*M against NO production. The other compounds (**1**−**4**, **6**−**9**, and **11**−**13**) exhibited moderate to weak inhibitory activities, with IC_{50}'s from 23.50 to 80.35 *μ*M.

The neuroprotective activity of compounds **1**−**13** was also evaluated by assessing their induction potentials on NGF secretion in C6 cells. Compound **13** (20 *μ*M) was a powerful stimulant of NGF release, carrying a stimulation level of 172.04 ± 5.18%, which was powerful when compared to the positive control 6-shogaol (143.74 ± 1.11%).

The cytotoxicity of compounds **1**−**13** was also gauged utilizing quantitative staining of cellular proteins by sulforhodamine B (SRB) against several cancer cell lines such as non-small-cell lung adenocarcinoma (A549), ovary malignant ascites (SK-OV-3), skin melanoma (SK-MEL-2), and breast carcinoma (Bt549).[24] All compounds tested were inactive (IC_{50} > 10 *μ*M) for the tested cancer cell lines in this study.

According to the present study delineating the identification of the new biflavonoids and their relevant biological activity, these active flavonoid-based compounds may be a reasonable pharmacophore for the development of anti-neurodegenerative agents given the predominant roles of NO and NGF in neuropathological conditions. This might also be supported by previous studies validating that flavonoid-based phytochemicals from the leaves of *Allium victorialis* var. *platyphyllum* and *Hosta longipes* displayed powerful inhibition of NO production.[25,26] Moreover, the current approach, investigating full structural details via application of new NMR techniques coupled with quantum-mechanics-based calculations, may be helpful in providing unambiguous assignments of highly functionalized flavonoids and/or molecules with low H/C ratios given the growing trend of misassigned structures being reported in the chemical literature.

DOI: 10.1021/acs.jnatprod.6b00981
J. Nat. Prod. XXXX, XXX, XXX−XXX

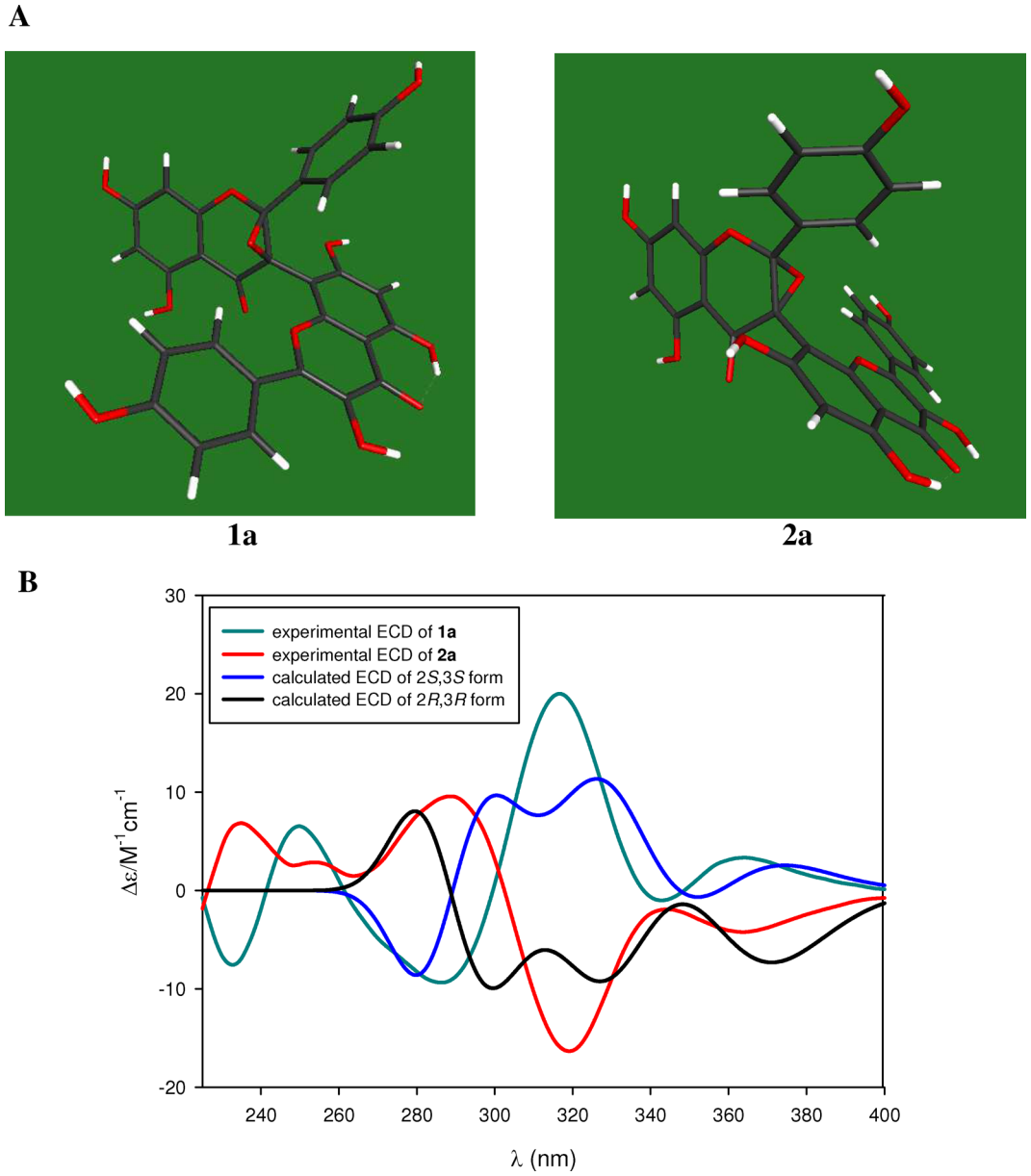

Figure 2. Determination of absolute configurations of compounds **1**−**4**. (A) 3D structures of **1a** and **2a**, which are the enzymatic hydrolysates of **1**/**3** and **2**/**4**, respectively. (B) Comparison of the experimental and computed ECD spectra of **1a** and **2a**.

EXPERIMENTAL SECTION

General Experimental Procedures. Optical rotation data were recorded utilizing a JASCO P-1020 polarimeter (JASCO, Easton, MD, USA). Infrared (IR) spectra were obtained utilizing a Bruker IFS-66/S Fourier-transform IR spectrometer (Bruker, Karlsruhe, Germany). Ultraviolet (UV) spectra were garnered using a Shimadzu UV-1601 UV−visible spectrophotometer (Shimadzu, Tokyo, Japan). The NMR studies were accomplished employing a Bruker AVANCE III 700 NMR spectrometer, and resultant spectra were processed using MestReNova (Mnova) 10.0 with default weighting functions. The relaxation delay of all the NMR experiments was 1 s. For the ^{1}H experiments, the acquisition time was 1.704 s, zero-filling was 32 k, the spectrum window was -2−14 ppm, and the 90 deg pulse was 6 μs at 55 dB. The ^{13}C experiments were performed with 0.865 s for the acquisition time, 64 k for the zero-filling, 0−200 ppm for the spectrum window, and 6.9 μs at 59 dB for the 90 deg pulse. The 2D NMR experiments adopted the spectra widths and 90 deg pulse values of the associated ^{1}H or ^{13}C experiments. The COSY experiments used the acquisition time of 0.15 s, the HSQC experiments employed the acquisition time of 0.15 s and one bond $^{1}J_{CH}$ value of 146 Hz, and the HMBC experiments utilized the acquisition time of 0.15 s and the $^{3}J_{CH}$ value of 8 Hz. The LR-HSQMBC pulse sequence was conducted with the t1 increments (indirect dimension) of 640 to evolve long-range heteronuclear correlations with the $^{n}J_{CH}$ value being optimized to 2 Hz (a transfer delay of 250 ms). The acquisition time was 0.15 s, and the BIRD $^{1}J_{CH}$ filter was used as the default of the new NMR experiment.[13,27] HRFABMS data were acquired on a Waters SYNAPT G2 (Milford, MA, USA). Fractionation and purification were achieved using a semipreparative HPLC system equipped with a Gilson 306 pump (Middleton, WI, USA) and a Shodex refractive index detector (New York, NY, USA). Low-pressure liquid chromatography (LPLC) was performed with a LiChroprep Lobar-A column packed with RP-C_{18} resins (Merck, Darmstadt, Germany) and an FMI QSY-0 pump. Open columns packed with silica gel 60 (70−230 and 230−400 mesh; Merck) or RP-C_{18} silica gel (Merck, 230−400 mesh) were implemented in crude fractionation and separation. Precoated silica gel F_{254} plates and RP-18 F_{254s} plates (Merck) were utilized for thin-layer chromatography (TLC). Absorbance of cells was assessed utilizing a microplate reader (Emax, Molecular Devices, Sunnyvale,

DOI: 10.1021/acs.jnatprod.6b00981
J. Nat. Prod. XXXX, XXX, XXX−XXX

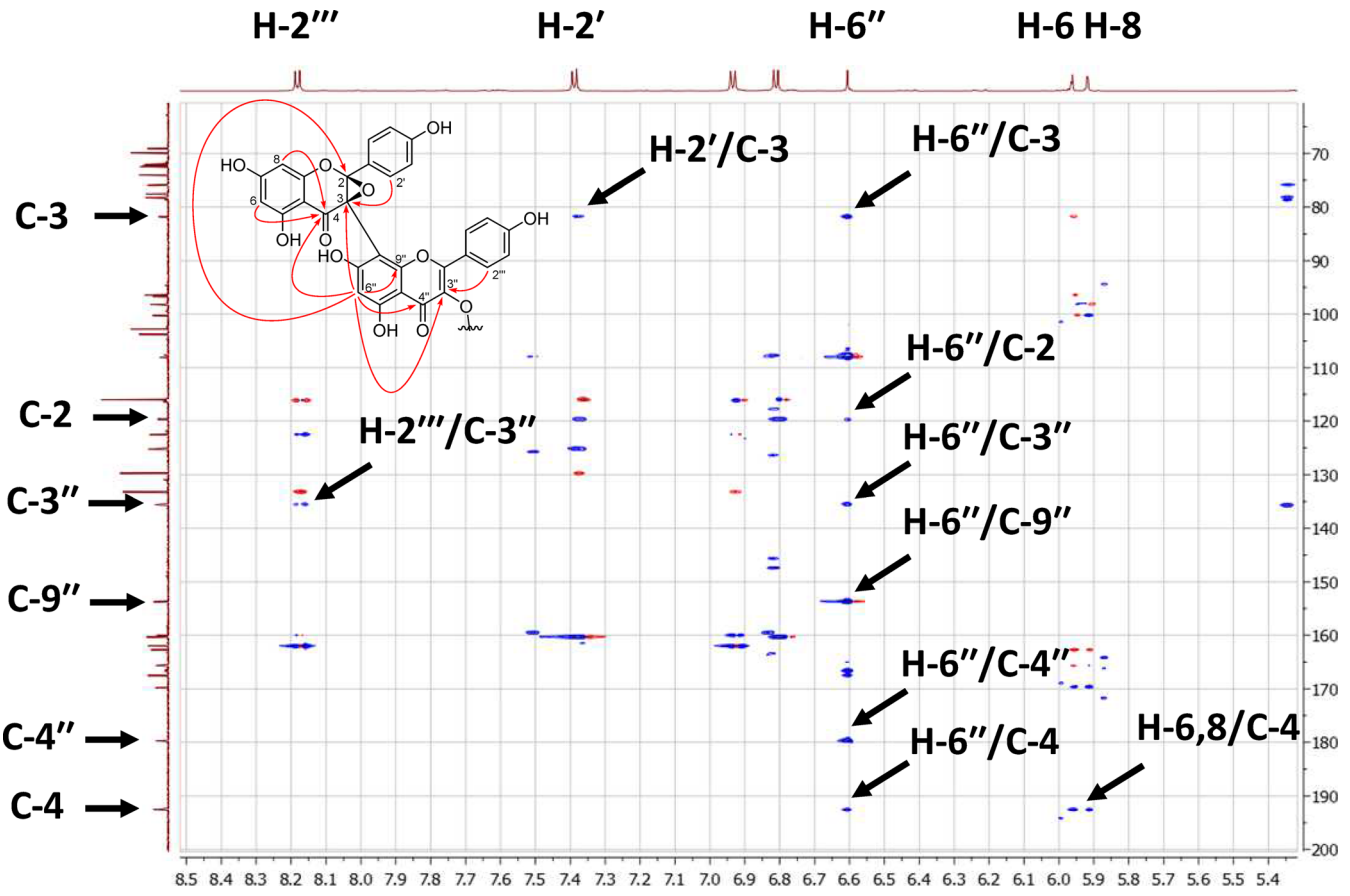

Figure 3. LR-HSQMBC cross-peaks of **3** in methanol-d_4.

Table 2. Inhibitory Effect of Compounds 1−13 on NO Production in LPS-Activated BV-2 Cells

compound	IC_{50} (μM)[a]	cell viability (%)[b]
1	33.33	110.29 ± 5.12
2	56.86	104.23 ± 5.04
3	39.16	99.88 ± 2.11
4	31.02	100.29 ± 4.68
5	8.86	118.57 ± 10.74
6	23.50	97.48 ± 2.95
7	31.73	102.51 ± 0.44
8	44.44	97.91 ± 2.97
9	80.35	97.54 ± 3.42
10	19.11	101.09 ± 4.50
11	55.59	95.61 ± 0.55
12	24.29	99.15 ± 3.44
13	32.66	96.97 ± 1.42
L-NMMA[c]	21.25	120.05 ± 11.65

[a]IC_{50} value of each compound was defined as the concentration (μM) that caused 50% inhibition of NO production in LPS-activated BV-2 cells. [b]Cell viability following treatment with 20 μM of each compound was determined using the MTT assay and is expressed as a percentage (%). Data are expressed as the mean ± standard deviation (SD) of three independent experiments. [c]Positive control.

CA, USA), and chemicals were purchased from Sigma-Aldrich (St. Louis, MO, USA).

Plant Material. The white flowers of *I. balsamina* were harvested in Asan, Republic of Korea, in August 2014. The detailed information can be found in an earlier communication.[12]

Extraction and Isolation. The details of the extraction method are elaborated in a previous study.[12] The EtOAc-soluble fraction (20 g) was subjected to normal-phase open column chromatography (silica; $CHCl_3$−MeOH−H_2O, 4:1:0.1) to generate eight fractions (fractions A−H). Fraction D (3.4 g) was chromatographed on a reversed-phase open column (RP-C_{18} silica; 60% aqueous MeOH) to afford six subfractions (fractions D1−D6). Among these, fraction D1 (170 mg) was separated using LPLC on a Lobar-A RP-C_{18} column (MeOH−H_2O, 2.5:7.5) followed by semipreparative HPLC (2 mL/min; MeOH−H_2O, 4:6) to obtain **13** (8 mg). Compounds **1** (10 mg), **2** (3 mg), **6** (20 mg), and **10** (6 mg) were furnished upon purification with a Lobar-A RP-C_{18} column (MeOH−H_2O, 1:1) followed by the semipreparative HPLC application (2 mL/min; MeOH−H_2O, 6.4:3.6). Fraction D4 (300 mg) was subjected to semipreparative HPLC (2 mL/min; MeOH−H_2O, 6:4) to afford **5** (18 mg). Fractions E1−E9 were obtained after RP-C_{18} silica gel open column chromatography (MeOH−H_2O, 5.5:4.5) from fraction E (1.5 g). Fractions E3 (50 mg), E4 (50 mg), E5 (490 mg), and E6 (260 mg) were purified using semipreparative HPLC (2 mL/min; 45−60% MeOH in H_2O) to afford **7** (6 mg), **11** (23 mg), **8** (130 mg), **3** (20 mg), and **4** (7 mg). Fraction F1 (1.0 g) was applied to a reversed-phase open column (RP-C_{18} silica; MeOH−H_2O, 5.5:4.5), and semipreparative HPLC (2 mL/min; MeOH−H_2O, 2:8) was performed to furnish **9** (6 mg) and **12** (6 mg).

*Balsamiside A (**1**):* yellowish gum; $[\alpha]_D^{25}$ +98 (*c* 0.2, MeOH); IR (KBr) ν_{max} cm^{-1} 3340, 2921, 1638, 1460, 1310, 1184; UV (MeOH) λ_{max} (log ε) 378 (3.40), 298 (3.60), 268 (3.65), 232 (4.35) nm; ECD (MeOH) λ_{max} ($\Delta\varepsilon$) 365 (+0.63), 315 (+6.01), 283 (−2.64), 249 (+1.28), 233 (−1.94), 217 (+2.69) nm; ^1H (700 MHz) and ^{13}C NMR (175 MHz) data, see Table 1; HRFABMS (negative-ion mode) *m*/*z* 731.1243 $[M - H]^-$ (calcd for $C_{36}H_{27}O_{17}$, 731.1243).

*Balsamiside B (**2**):* yellowish gum; $[\alpha]_D^{25}$ −98 (*c* 0.1, MeOH); IR (KBr) ν_{max} cm^{-1} 3339, 2922, 1638, 1460, 1311, 1183; UV (MeOH) λ_{max} (log ε) 380 (3.45), 299 (3.58), 265 (3.66), 232 (4.29) nm; ECD

DOI: 10.1021/acs.jnatprod.6b00981
J. Nat. Prod. XXXX, XXX, XXX−XXX

(MeOH) λ_{max} ($\Delta\varepsilon$) 364 (−1.28), 317 (−5.98), 280 (+2.66), 236 (+2.65), 218, (−3.44) nm; ^{1}H (700 MHz) and ^{13}C NMR (175 MHz) data, see Table 1; HRFABMS (negative-ion mode) m/z 731.1242 [M − H]$^-$ (calcd for $C_{36}H_{27}O_{17}$, 731.1243).

*Balsamiside C (**3**):* yellowish gum; $[\alpha]_D^{25}$ +88 (c 0.9, MeOH); IR (KBr) ν_{max} cm^{-1} 3339, 2923, 1636, 1457, 1310, 1180; UV (MeOH) λ_{max} (log ε) 377 (3.43), 297 (3.59), 266 (3.68), 234 (4.32) nm; ECD (MeOH) λ_{max} ($\Delta\varepsilon$) 364 (+1.05), 317 (+6.25), 286 (−2.92), 250 (+2.04), 233 (−2.36), 217, (+2.15) nm; ^{1}H (700 MHz) and ^{13}C NMR (175 MHz) data, see Table 1; HRFABMS (negative-ion mode) m/z 877.1821 [M − H]$^-$ (calcd for $C_{42}H_{37}O_{21}$, 877.1822).

*Balsamiside D (**4**):* yellowish gum; $[\alpha]_D^{25}$ −61 (c 0.4, MeOH); IR (KBr) ν_{max} cm^{-1} 3339, 2920, 1638, 1458, 1311, 1180; UV (MeOH) λ_{max} (log ε) 380 (3.40), 297 (3.56), 267 (3.67), 232 (4.18) nm; ECD (MeOH) λ_{max} ($\Delta\varepsilon$) 364 (−1.56), 319 (−6.05), 289 (+3.55), 235 (−2.54), 218 (−3.20) nm; ^{1}H (700 MHz) and ^{13}C NMR (175 MHz) data, see Table 1; HRFABMS (negative-ion mode) m/z 877.1823 [M − H]$^-$ (calcd for $C_{42}H_{37}O_{21}$, 877.1822).

Acid Hydrolysis of 1−4. Compounds **1**−**4** (1.0 −2.0 mg) were hydrolyzed with 1 N HCl (1 mL) under reflux for 2 h. EtOAc was used to extract the organic layers from each reaction mixture, and the organic extracts were concentrated to produce 0.5−1.0 mg of **1a** (from **1** and **3**) and **2a** (from **2** and **4**). The monosaccharide residue was acquired from the H_2O-soluble phase upon neutralization via an Amberlite IRA-67 column.

*[(2S,3S)-2,3-Epoxy-5,7,4′-trihydroxyflavanone]-(3→8)-kaempferol (**1a**):* yellowish gum; $[\alpha]_D^{25}$ +215 (c 0.1, MeOH); ECD (MeOH) λ_{max} ($\Delta\varepsilon$) 363 (+1.11), 317 (+6.30), 286 (−2.99), 249 (+1.95), 233 (−2.30), 216, (+2.12) nm; ^{1}H NMR (methanol-d_4, 700 MHz) δ 8.28 (2H, d, J = 8.9 Hz, H-2‴ and H-6‴), 7.40 (2H, d, J = 8.8 Hz, H-2′ and H-6′), 6.94 (2H, d, J = 8.9 Hz, H-3‴ and H-5‴), 6.80 (2H, d, J = 8.8 Hz, H-3′ and H-5′), 6.57 (1H, s, H-6″), 5.82 (1H, d, J = 2.1 Hz, H-6 or H-8), 5.78 (1H, d, J = 2.1 Hz, H-6 or H-8); FABMS (positive-ion mode) m/z 571.2 [M + H]$^+$.

*[(2R,3R)-2,3-Epoxy-5,7,4′-trihydroxyflavanone]-(3→8)-kaempferol (**2a**):* yellowish gum; $[\alpha]_D^{25}$ −220 (c 0.1, MeOH); ECD (MeOH) λ_{max} ($\Delta\varepsilon$) 364 (−1.60), 319 (−6.11), 288 (+3.40), 235 (−2.50), 218 (−3.05) nm; ^{1}H NMR (= **1a**); FABMS (positive-ion mode) m/z 571.2 [M + H]$^+$.

Establishment of Absolute Configuration of Sugar Moieties of Compounds 1−4. The monosaccharides, obtained after the hydrolysis of **1**−**4**, were added to anhydrous pyridine (0.5 mL) containing L-cysteine methyl ester hydrochloride (2 mg). The reaction mixture was kept at 60 °C for 1.5 h and derivatized with 1-trimethylsilylimidazole (0.1 mL) for 2 h. Each reaction mixture was extracted using n-hexane and H_2O (1 mL each), and the n-hexane phase (1 μL) was subjected to GC/MS analysis.[18] The monosaccharides D-glucose and L-rhamnose were identified upon co-injection of the hydrolysates with the silylated standards, providing a peak at 9.857 min (D-glucose) and 6.320 min (L-rhamnose). The authentic compounds, derivatized in the identical manner, exhibited peaks at 9.852 min (D-glucose), 10.531 min (L-glucose), 6.323 min (L-rhamnose), and 6.078 min (D-rhamnose), respectively.

Computational Analysis. The optimization of geometries was achieved at the B3LYP/DFT level with the basis set def-SV(P) using Turbomole 6.5. With reference to a previous study, the ECD spectra were simulated using the equation shown below.[28] The bandwidth (σ) of 0.10 eV was used for this study.

$$\Delta\varepsilon(E) = \frac{1}{2.297 \times 10^{-39}} \frac{1}{\sqrt{2\pi}\sigma} \sum_{t}^{A} \Delta E_i R_i e^{[-(E-\Delta E_i)^2/(2\sigma)^2]}$$

Assessment of NO Generation and Cell Viability. BV-2 cells, developed by Dr. V. Bocchini at the University of Pergia (Pergia, Italy), were used for this study. The cells were seeded in a 96-well plate (4×10^4 cells/well) and incubated in the presence or absence of various doses of test compounds. LPS (100 ng/mL) was added to BV-2 cells and grown for 1 d. The produced levels of nitrite (NO_2), a soluble oxidized product of NO, were evaluated with 0.1% N-1-naphthylethylenediamine dihydrochloride and 1% sulfanilamide in 5% phosphoric acid, aka the Gries reagent. The supernatant (50 μL) was mixed with the Gries reagent (50 μL). After 10 min the absorbance was gauged at 570 nm. For a positive control, the reported nitric oxide synthase inhibitor L-NMMA was employed. Graded sodium nitrite solution was utilized to determine nitrite concentrations. An MTT assay was used for the cell viability assay.

NGF and Cell Viability Assays. The C6 cells (Korean Cell Line Bank, Seoul, Republic of Korea) were seeded in a 24-well plate at 1×10^5 cells/well. After 1 d, the cells were applied with serum-free DMEM and various doses of the phytochemicals for another day. From the cultured plates, the medium supernatant was collected and the changes in NGF release were measured utilizing an ELISA kit. The viability of the C6 cells was evaluated via an MTT assay. The outcomes were shown as a percentage compared to the negative control (i.e., untreated cells). The positive control was 6-shogaol.

Cytotoxicity Assessment. The cytotoxicity of purified metabolites against the four aforementioned human tumor cell lines was evaluated by an SRB method.[24] Etoposide (≥98%; Sigma-Aldrich) served as a positive control, which exhibited the respective IC_{50}'s of 0.92, 1.95, 1.10, and 1.24 μM against A549, SK-OV-3, SK-MEL-2, and Bt549.

Table 3. Effects of Compounds 1−13 on NGF Secretion in C6 Cells

compound	NGF secretion[a] (%)	cell viability[b] (%)
1	121.42 ± 5.99	112.92 ± 6.98
2	90.12 ± 4.61	107.18 ± 5.58
3	88.36 ± 0.48	102.21 ± 6.72
4	74.27 ± 2.33	109.14 ± 6.50
5	115.98 ± 3.08	97.22 ± 1.03
6	114.67 ± 13.17	114.67 ± 5.05
7	123.31 ± 14.75	102.28 ± 5.73
8	97.59 ± 10.69	99.59 ± 0.74
9	83.79 ± 9.45	105.18 ± 6.23
10	118.77 ± 10.96	102.83 ± 0.34
11	98.67 ± 12.25	106.54 ± 5.56
12	108.27 ± 20.45	112.58 ± 8.26
13	172.04 ± 5.18	109.58 ± 4.12
6-shogaol[c]	143.74 ± 1.11	103.83 ± 10.86

[a]C6 cells were treated with 20 μM of each compound. After 24 h, the content of NGF secreted in the C6-conditioned medium was measured by ELISA. The level of secreted NGF is expressed as the percentage of the untreated control (set as 100%). [b]Cell viability after treatment with 20 μM of each compound was determined by an MTT assay and is expressed as a percentage (%). Results are the means of three independent experiments, and the data are expressed as mean ± SD. [c]Positive control.

■ ASSOCIATED CONTENT

Supporting Information

The Supporting Information is available free of charge on the ACS Publications website at DOI: 10.1021/acs.jnatprod.6b00981.

HRFABMS, NMR, and ECD information on compounds **1**−**4** and ^{1}H NMR data of **1a** (=**2a**) (PDF)

■ AUTHOR INFORMATION

Corresponding Author

*Tel: 82-31-290-7710. Fax: 82-31-290-7730. E-mail: krlee@skku.edu.

ORCID

Dong-Chan Oh: 0000-0001-6405-5535

Kang Ro Lee: 0000-0002-3725-5192

DOI: 10.1021/acs.jnatprod.6b00981
J. Nat. Prod. XXXX, XXX, XXX−XXX

Notes

The authors declare no competing financial interest.

■ ACKNOWLEDGMENTS

The current study was made possible through research funding from the Dong-A ST Research Center, 2015. We are grateful to the Korea Basic Science Institute (KBSI) for the mass spectroscopic analyses.

■ REFERENCES

(1) Imam, M. Z.; Nahar, N.; Akter, S.; Rana, M. S. *J. Ethnopharmacol.* **2012**, *142*, 804−810.
(2) Hu, X.-I.; Han, Z.-X.; Liu, Y.-F.; Zhao, H.; Li, Y.-L.; Mao, N.-W. *Food Sci.* **2007**, *28*, 48−49.
(3) Herrera, A. A.; Ocampo, M. A. B.; Guevara, A. P. *J. Med. Plants Res.* **2013**, *7*, 2846−2858.
(4) Fukumoto, H.; Yamaki, M.; Isoi, K.; Ishiguro, K. *Phytother. Res.* **1996**, *10*, 202−206.
(5) Ishiguro, K.; Oku, H. *Phytother. Res.* **1997**, *11*, 343−347.
(6) Oku, H.; Ishiguro, K. *Biol. Pharm. Bull.* **2002**, *25*, 658−660.
(7) Shanmugam, K.; Holmquist, L.; Steele, M.; Stuchbury, G.; Berbaum, K.; Schulz, O.; Benavente García, O.; Castillo, J.; Burnell, J.; Garcia Rivas, V. *Mol. Nutr. Food Res.* **2008**, *52*, 427−438.
(8) Cho, J. *Arch. Pharmacal Res.* **2006**, *29*, 699−706.
(9) Yin, L.-L.; Lin, L.-L.; Zhang, L.; Li, L. *Neuropharmacology* **2012**, *63*, 851−862.
(10) Dawson, T. M.; Dawson, V. L.; Snyder, S. H. *Ann. Neurol.* **1992**, *32*, 297−311.
(11) Wyman, T.; Rohrer, D.; Kirigiti, P.; Nichols, H.; Pilcher, K.; Nilaver, G.; Machida, C. *Gene Ther.* **1999**, *6*, 1648−1660.
(12) Kim, C. S.; Subedi, L.; Kim, S. Y.; Choi, S. U.; Choi, S. Z.; Son, M. W.; Kim, K. H.; Lee, K. R. *Phytochem. Lett.* **2015**, *14*, 215−220.
(13) Williamson, R. T.; Buevich, A. V.; Martin, G. E.; Parella, T. *J. Org. Chem.* **2014**, *79*, 3887−3894.
(14) Ramos, F. A.; Takaishi, Y.; Shirotori, M.; Kawaguchi, Y.; Tsuchiya, K.; Shibata, H.; Higuti, T.; Tadokoro, T.; Takeuchi, M. *J. Agric. Food Chem.* **2006**, *54*, 3551−3557.
(15) Ding, Y.; Li, X.-C.; Ferreira, D. *J. Nat. Prod.* **2008**, *72*, 327−335.
(16) Ding, Y.; Li, X.-C.; Ferreira, D. *J. Org. Chem.* **2007**, *72*, 9010−9017.
(17) Liu, J.; Wu, H.; Zheng, F.; Liu, W.; Feng, F.; Xie, N. *J. Sep. Sci.* **2014**, *37*, 2513−2522.
(18) Kim, C. S.; Kwon, O. W.; Kim, S. Y.; Kim, K. H.; Lee, K. R. *Heterocycles* **2014**, *89*, 1913−1922.
(19) Markham, K.; Ternai, B.; Stanley, R.; Geiger, H.; Mabry, T. *Tetrahedron* **1978**, *34*, 1389−1397.
(20) Kazuma, K.; Noda, N.; Suzuki, M. *Phytochemistry* **2003**, *62*, 229−237.
(21) Okuyama, T.; Hosoyama, K.; Hiraga, Y.; Jurono, G.; Takemono, T. *Chem. Pharm. Bull.* **1978**, *26*, 3071−3074.
(22) Li, Y.-L.; Li, J.; Wang, N.-L.; Yao, X.-S. *Molecules* **2008**, *13*, 1931−1941.
(23) Jeon, S. H.; Chun, W.; Choi, Y. J.; Kwon, Y. S. *Arch. Pharm. Res.* **2008**, *31*, 978−982.
(24) Skehan, P.; Storeng, R.; Scudiero, D.; Monks, A.; McMahon, J.; Vistica, D.; Warren, J. T.; Bokesch, H.; Kenney, S.; Boyd, M. R. *J. Natl. Cancer Inst.* **1990**, *82*, 1107−1112.
(25) Woo, K. W.; Moon, E.; Park, S. Y.; Kim, S. Y.; Lee, K. R. *Bioorg. Med. Chem. Lett.* **2012**, *22*, 7465−7470.
(26) Kim, C. S.; Kwon, O. W.; Kim, S. Y.; Lee, K. R. *J. Braz. Chem. Soc.* **2014**, *25*, 907−912.
(27) Saurí, J.; Liu, Y.; Parella, T.; Williamson, R. T.; Martin, G. E. *J. Nat. Prod.* **2016**, *79*, 1400−1406.
(28) Kim, C. S.; Shin, B.; Kwon, O. W.; Kim, S. Y.; Choi, S. U.; Oh, D.-C.; Kim, K. H.; Lee, K. R. *Tetrahedron Lett.* **2014**, *55*, 6504−6507.

DOI: 10.1021/acs.jnatprod.6b00981
J. Nat. Prod. XXXX, XXX, XXX−XXX